



# Direct adiabatic cooling systems – Resilience to climate change for industrial building applications in a Mediterranean climate

Antoine Breteau, Patrick Salagnac, Jean-Marie Caous, Emmanuel Bozonnet

## ► To cite this version:

Antoine Breteau, Patrick Salagnac, Jean-Marie Caous, Emmanuel Bozonnet. Direct adiabatic cooling systems – Resilience to climate change for industrial building applications in a Mediterranean climate. AIVC - Retrofitting the Building Stock: Challenges and Opportunities for Indoor Environmental Quality, Oct 2024, Dublin, Ireland. hal-04636838

**HAL Id: hal-04636838**

**<https://hal.science/hal-04636838>**

Submitted on 5 Jul 2024

**HAL** is a multi-disciplinary open access archive for the deposit and dissemination of scientific research documents, whether they are published or not. The documents may come from teaching and research institutions in France or abroad, or from public or private research centers.

L'archive ouverte pluridisciplinaire **HAL**, est destinée au dépôt et à la diffusion de documents scientifiques de niveau recherche, publiés ou non, émanant des établissements d'enseignement et de recherche français ou étrangers, des laboratoires publics ou privés.



Distributed under a Creative Commons Attribution - NonCommercial - NoDerivatives 4.0 International License

# Direct adiabatic cooling systems – Resilience to climate change for industrial building applications in a Mediterranean climate

Antoine Breteau<sup>\*1, 2</sup>, Patrick Salagnac<sup>1</sup>, Jean-Marie Caous<sup>2</sup>, Emmanuel Bozonnet<sup>1</sup>

*1 LaSIE (UMR 7356), La Rochelle Université  
Av.M.Crépeau, La Rochelle  
17042, France*

*2 BLUETEK  
Z.I Nord les Pins, Luynes  
17042, France*

*\*Corresponding author: [antoine.breteau@univ-lr.fr](mailto:antoine.breteau@univ-lr.fr)*

## ABSTRACT

This paper presents an analysis of the resilience to climate change of a direct adiabatic cooling system integrated within an industrial building. The system is a solution that utilizes humidified porous material to lower the air temperature without requiring external energy. In this study, the system is evaluated for two typical climate periods (historical and future) for a Mediterranean climate, using indicators of energy performance, thermal comfort and water consumption. The results reveal that compared to the reference case, the system reduces indoor overheating almost similarly between the typical historical climate (76%) and typical future climate (71%). In addition, climate change would increase total system energy consumption by 40% and double water consumption. However, climate change increases the performance of the system, particularly with regard to the reduction of interior overheating in relation to the energy consumption of the fan (+90%) and the volume of water evaporated (+19%). To finish, the system is resilient in the face of climate change, even if this is 38% weaker between typical historical and future climate.

## KEYWORDS

Passive cooling, adiabatic cooling, comfort, resilience

## 1 INTRODUCTION

On 12 January 2024, the World Meteorological Organisation (WMO) officially declared that 2023 had been the warmest year on record. The average annual temperature across the world was 1.5 °C above pre-industrial levels (WMO 2024). Human activities are increasing the phenomenon of rising temperatures, particularly the intensive use of air conditioning. This solution, which is becoming increasingly popular for cooling buildings during heat peaks (Batiweb 2023), is also one of the problematic factors exacerbating global warming (Salamanca et al. 2014). Air conditioning accounts for 12% of the building sector's greenhouse gas emissions (PROMEE 2023). To tackle the impact of global warming and reduce the use of air conditioners, passive adiabatic cooling methods are being developed.

Adiabatic cooling is emerging as a promising solution to address environmental challenges, particularly in ensuring resilient building cooling amidst climate change, as suggested by the work of Annex 80 of the International Energy Agency (IEA) (Zhang et al. 2021). Unlike traditional air conditioners, this technology avoids the use of refrigerants and consumes considerably less electrical energy (Ford et al. 1998; McKenzie et al. 2013). Adiabatic cooling systems cool building interiors by harnessing the energy from water evaporation produced by the passage of hot, dry air through a wet porous material (Watt 1997). This isenthalpic process requires minimal external energy for the water pump and fan. Direct adiabatic systems supply cool and humid air to the building, while indirect adiabatic systems prevent moisture buildup

by using an air heat exchanger (Xuan et al. 2012). The combination of both direct and indirect approaches is more complex, though this allows to dynamically optimize the system performance (PROFEEL 2021).

These systems are particularly effective in hot, dry climates (Chiesa et al. 2017). Our previous studies have demonstrated the effectiveness of direct adiabatic systems in reducing overheating inside buildings (Breteau et al. 2022; 2023). In terms of energy performance, these systems are often considered as a robust and practical alternative for cooling industrial buildings, due to the low energy consumption of direct adiabatic systems (Kowalski et Kwiecień 2020), although water consumption is an aspect to be taken into account (Sahai 2012; Kowalski et Kwiecień 2020).

The aim of this paper is to examine the resilience of a direct adiabatic system integrated into an industrial building in response to climate change, specifically in a Mediterranean climate context. We compare the system performances for the both historical (before 2020) and mid-term (around 2050) periods. We then analyse the behavior of the system, highlighting the different operation phases. Finally, we give a detailed analysis of the direct adiabatic system performance, regarding thermal comfort and resilience indicators.

## 2 CASE STUDY

### 2.1 Typical industrial building

The building studied is a warehouse-type industrial building, consisting of a steel structure with a floor area of  $36 \times 36 \text{ m}^2$  and a height of 8 m (Figure 1).

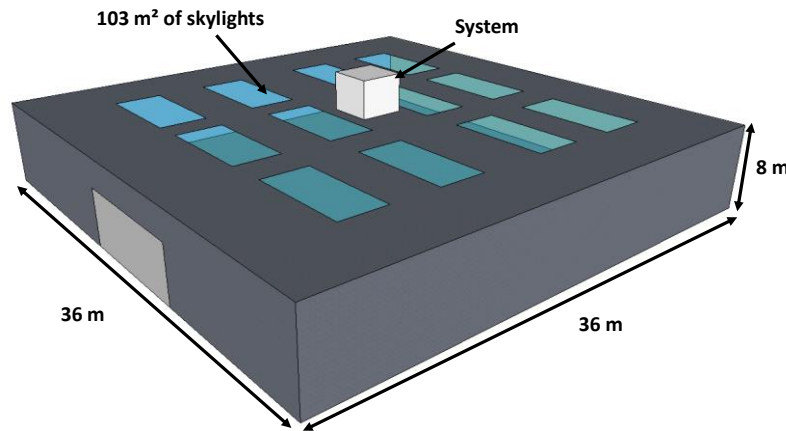


Figure 1 : Geometry of the industrial building

The building stores merchandises (paperboard, metal and pallets box) on metal shelves whose inertia is considered as an internal mass. The vertical walls and roof are made up of two 2 mm thick steel claddings covering a 5 cm thick layer of rock wool. The floor consists of an uninsulated 20 cm concrete slab. The building has  $103 \text{ m}^2$  of skylights evenly distributed across the roof (8% of the roof surface). The building has an air permeability equivalent to  $2.6 \text{ m}^3 \cdot \text{h}^{-1} \cdot \text{m}^{-2}$  (under 4 Pa) without a ventilation system, but a hygienic flow rate of  $45 \text{ m}^3 \cdot \text{h}^{-1} \cdot \text{occ}^{-1}$  has been set up to comply with standards. It is designed to accommodate an occupancy density of  $60 \text{ m}^2 \cdot \text{occ}^{-1}$  during opening hours, from 7 a.m to 10 p.m. every day except Sunday. For ventilation and cooling, the building uses a direct adiabatic cooling system.

## 2.2 Direct evaporative cooling system

We have developed a numerical model and integrated into the thermal simulation software for buildings (TRNSYS©) based on the saturation efficiency  $\epsilon_{wb}$ , see equation (1).

$$\epsilon_{wb} = 100 \frac{T_{AO} - T_{AS}}{T_{AO} - T_{wb,AO}} \quad (1)$$

with  $T_{AO}$ ,  $T_{AS}$ , and  $T_{wb,AO}$  respectively the outside air temperature, the supply air temperature and the wet bulb temperature of the outside air.

The system reduces the dry bulb temperature of the outside air to its wet bulb temperature by means of the energy of evaporation of the water produced as the air passes through a porous material.

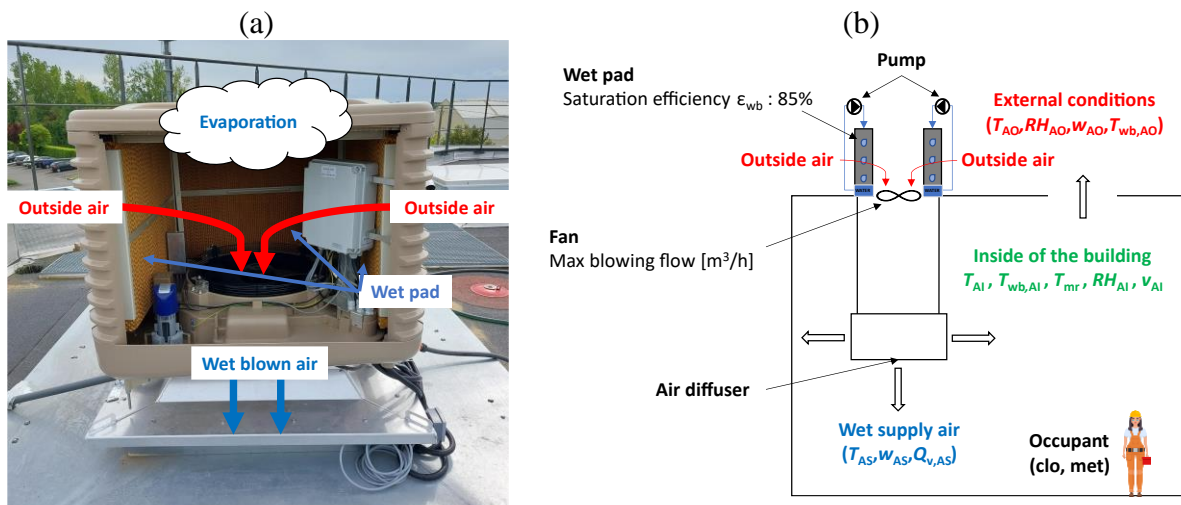


Figure 2 : direct adiabatic system (a), and system integration onto the building (b)

An adiabatic box (Figure 2) is composed of several wet media with a saturation efficiency of 85%, a fan (12 000 m<sup>3</sup>/h for this box), and a water pump. This box is installed on the roof of the building (Figure 2), and can operate either in free-cooling mode (fan only), or in adiabatic mode (with humidification). The regulation of both modes of the system remains similar, where the fan adjusts its airflow based on a proportional band of 2 °C with different temperature conditions (Table 1).

Table 1 : Indoor and outdoor temperature conditions

Air temperature conditions	Free cooling conditions		Adiabatic conditions	
	Indoor ( $T_{AI}$ )	Outdoor ( $T_{AO}$ )	Indoor ( $T_{AI}$ )	Outdoor ( $T_{wb,AO}$ )
Occupancy hours	> 22 °C	< $T_{AI}$	> 24 °C	< $T_{AI}$
Unoccupied hours	> 19 °C	< $T_{AI}$	> 28 °C	< $T_{AI}$

In free-cooling mode, this proportional band applies between the indoor temperature ( $T_{AI}$ ) and a set indoor target temperature, as well as the outdoor temperature ( $T_{AO}$ ). In adiabatic mode, however, the proportional band applies between the indoor temperature ( $T_{AI}$ ) and a target temperature, and also with the outdoor wet-bulb temperature ( $T_{wb,AO}$ ). This control makes it possible to optimise the use of the cooling potential offered between the outdoor and indoor conditions.

In this study, the resilience of the system was assessed regarding the historical climate (1990 – 2019) versus the mid-term climate change (2040 – 2069). We used the typical weather files (TMY) generated from the hourly historical weather data and the mid-term future climate from Cordex data (Machard et al. 2020). The method considers the high emissions scenario for future climate change.

The sizing of the direct adiabatic system is crucial for our study in terms of energy performance in dynamic mode, and is highly dependent on the location of the building. To this end, we determined the optimum steady-state airflow rate, taking into account typical outdoor conditions for the climate studied and the equivalent indoor temperature ( $SET^*$ ) obtained from different airflow rates of the direct adiabatic system. As the efficiency of the system is not 100%, the cooling effect tends towards an asymptotic ideal value, and we have chosen the cooling effect of 2/3 to define the maximum fan airflow rate. Sizing the system for a Mediterranean climate (Carpentras) resulted in a maximum airflow of 22 000 m<sup>3</sup>/h (2.1 ACH).

### 2.3 Key Performance Indicators (KPI)

In this article, various comfort, performance and resilience indicators were used. To assess indoor thermo(hydric) comfort, the  $T_{op}$  and  $SET^*$  indicators were chosen.

The  $SET^*$  temperature is defined as an operating temperature of a reference environment that would cause the same physiological responses as the real environment. The  $SET^*$  is defined as the equivalent of the dry temperature of an isothermal environment at 50% relative humidity where the occupants would have standardised clothing for the activity under consideration, which would have the same thermal constraint (skin temperature) and the same thermoregulatory constraint (skin humidity) as in a reference environment (Gagge, Fobelets, et Berglund 1986).

Indoor thermo(hydric) discomfort was assessed by the number of degree-hours above the limit temperature ( $T_{i,lim}$ ).  $T_{i,lim}$  values for  $T_{op}$  and  $SET^*$  were determined by an equivalence method using the PMV indicator (Zare et al. 2018). We chose a PMV indicator equal to 0 (neutral thermal sensation) and the following parameters:  $v_{AI} = 0.2$  m/s; metabolism 1.4 met; clothing 0.5 clo. According to the psychrometric comfort diagram (ASHRAE 2013), an operating temperature  $T_{op}$  of 26 °C has a  $SET^*$  equivalence of 28 °C.

The system's performance was assessed using indicators to reduce internal overheating, based on water consumption ( $\Delta SETH/V_w$ ) (2) and fan energy consumption ( $\Delta SETH/C_{fan}$ ) (3).

$$\frac{\Delta SETH}{V_w} = \frac{SETH_{ref} - SETH_{sys}}{V_w} \quad (2)$$

$$\frac{\Delta SETH}{C_{fan}} = \frac{SETH_{ref} - SETH_{sys}}{C_{fan}} \quad (3)$$

with  $\Delta SETH$ ,  $C_{fan}$  and  $V_w$  respectively the reduction in internal overheating by the system, the fan energy consumption and the volume of water evaporated.

The system resilience was analysed using the  $\alpha$  indicator, which assesses a building ability to withstand the impacts of climate change and the resulting risk of overheating (4). This is determined by the slope of the regression between the  $IOD$  and the  $AWD$  (Hamdy et al. 2017).  $IOD$  quantifies interior overheating relative to a limit ( $T_{lim} = 26$  °C) and  $AWD$  is used to quantify the severity of outdoor thermal conditions relative to a base temperature ( $T_b = 26$  °C).

$$\alpha = \frac{IOD}{AWD} \quad (4)$$

If  $\alpha < 1$  then the building is able to eliminate external thermal stress in the long term and if  $\alpha > 1$  then the building is unable to eliminate external thermal stress in the long term.

### 3 RESULTS AND DISCUSSIONS

#### 3.1 Climate data

Climate data (temperature and relative humidity) of the historical (left) and future (right) climate are displayed on a heatmap with the days on the x-axis and the times of day on the y-axis (Figure 3).

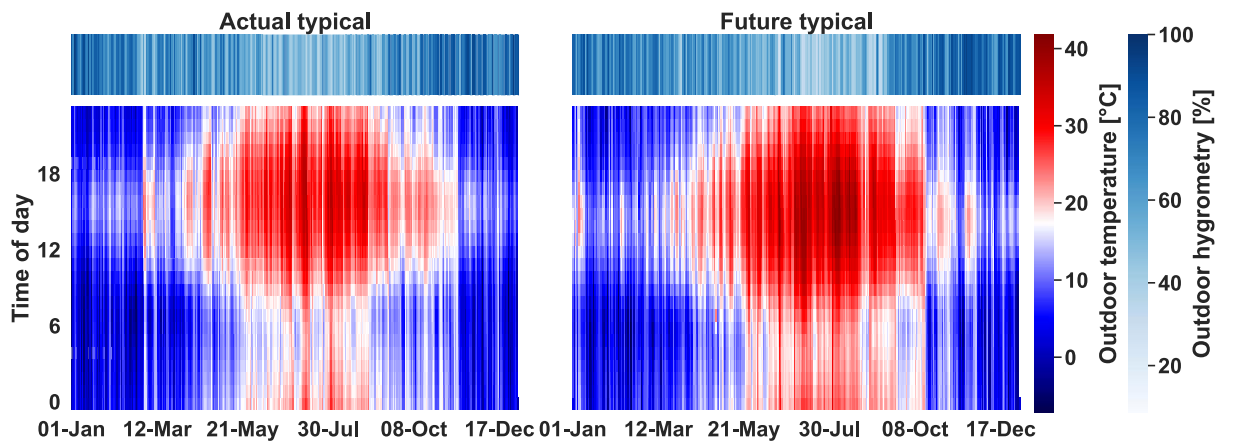


Figure 3 : Outdoor conditions

Figure 3 shows the disparity between historical and future climate. The analysis reveals an increase in night-time temperatures in the future climate scenario compared with historical data. Although the seasonal trend remains stable, with periods of intense heat from late May to early October, the average annual temperature rises significantly in the future scenario, showing an increase of 2 °C. Maximum temperatures rise from 37 °C in the historical period to 41 °C in the future period. At the same time, average relative humidity over the year falls by 2 points in the future scenario.

#### 3.2 System operation

The study examined the behaviour of the system by analysing variations in water consumption and changes in free-cooling (green) and adiabatic (purple) operating modes over historical and future climate periods. These results are presented in the form of a heatmap showing the percentage of fan flow for each mode by color intensity as a function of time of day (y-axis) and day of year (x-axis) (Figure 4).

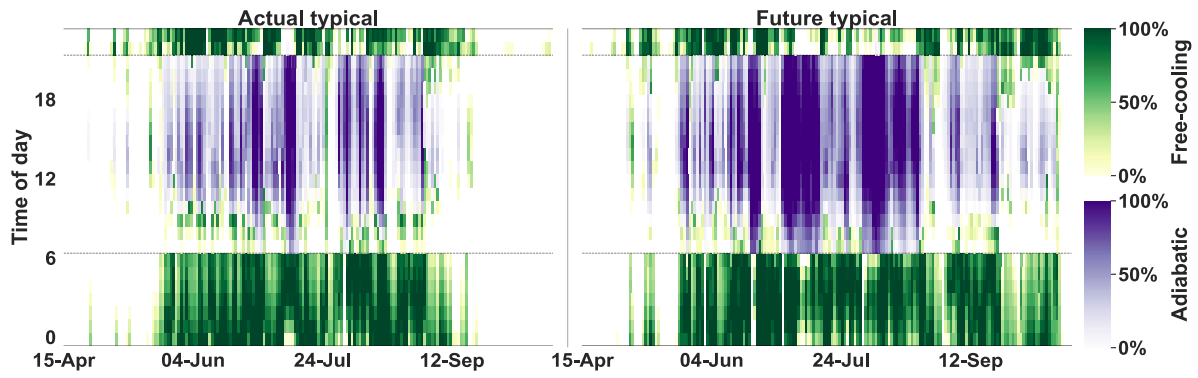


Figure 4 : The operation of both modes

Figure 4 indicates that free-cooling is generally used during periods when the building is not occupied, while adiabatic cooling is used during periods of occupancy, especially when free-cooling has not lowered the indoor temperature sufficiently. However, for the typical future period, the times when free-cooling was used during occupancy are now considered to be in adiabatic mode due to the increase in outdoor and indoor temperatures. Quantitatively, there was a 53% increase in the number of hours of operation in adiabatic mode and a 16% increase in free-cooling mode between the typical historical and future meteorological periods.

The increase in running time has led to significant changes in energy consumption. Pump consumption increased by 53%, from 43 kWh to 66 kWh, while total annual energy consumption increased by 40%, from 7 013 kWh to 9 812 kWh. The quantity of water evaporated more than doubled, from 75 m<sup>3</sup> to 161 m<sup>3</sup>. Including emptying cycles, it went from 143 m<sup>3</sup> to 220 m<sup>3</sup> per year.

### 3.3 Thermal comfort and system performance

Thermo(hydric) comfort was analysed using *SET\**. The results represent indoor overheating with a color gradient based on its intensity. The days of the year are depicted on the x-axis, and the hours of the day on the y-axis. For each climate period, the upper figure illustrates indoor overheating without the system, while the lower figure represents indoor overheating with the system (Figure 5).

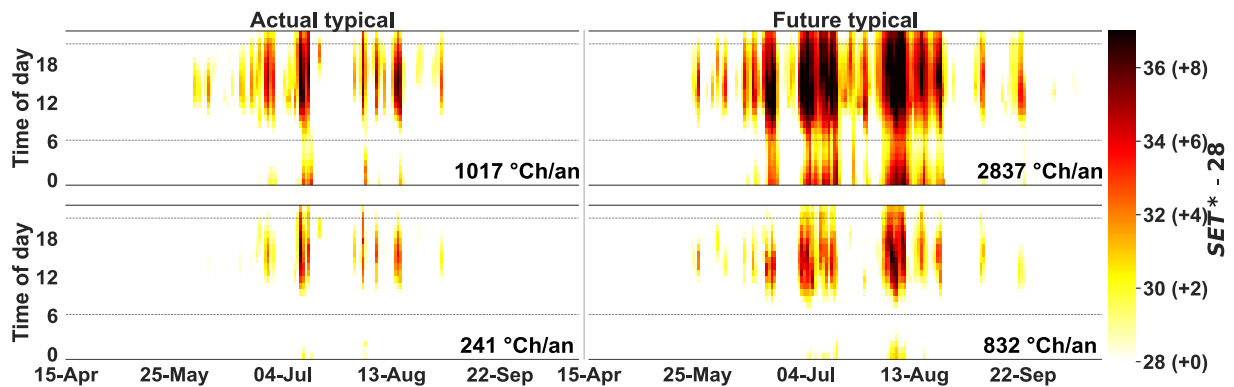


Figure 5 : Internal overheating ( $SET^* - SET^*_{lim}$ )

In the absence of the system, in a future climate, there is a clear increase in the duration and intensity of daily overheating periods, particularly in July and August. The number of degree hours in the future climate is almost three times that of the historical climate, largely due to external inputs. It is also notable that the system effect on reducing indoor discomfort decreases



according to future climate. The observed reduction is 76% (from 1 017 °Ch to 241 °Ch) for the historical climate, compared with 71% (from 2 837 °Ch to 818 °Ch) for the future period.

Then we compare the multiple aspects of the system performances for both typical historical and typical future climate, which we synthetized in a radar chart (Figure 6 - left) for the relative performances (reference without system 0%), and a table (Figure 6 - right) for the absolute performances (absolute values without system in brackets). The relative performance maxima (100%) have been specifically set for  $\Delta SETH/V_w$  and  $\Delta SETH/C_{fan}$  indicators, given the maximum performance that we obtained for these two indicators with the help of simulations in a set of various locations (historical and future climates). Hence, we obtained the maximum performance for Singapore location ( $\Delta SETH/V_w = 35.26$  °Ch/m<sup>3</sup>, and  $\Delta SETH/C_{fan} = 0.85$  °Ch/kWh) for Singapore. The other indicator maxima are consistent with the parameters, i.e., 100% performance in degree-hour ( $DH$ ) reduction means that  $DH = 0$  °Ch.

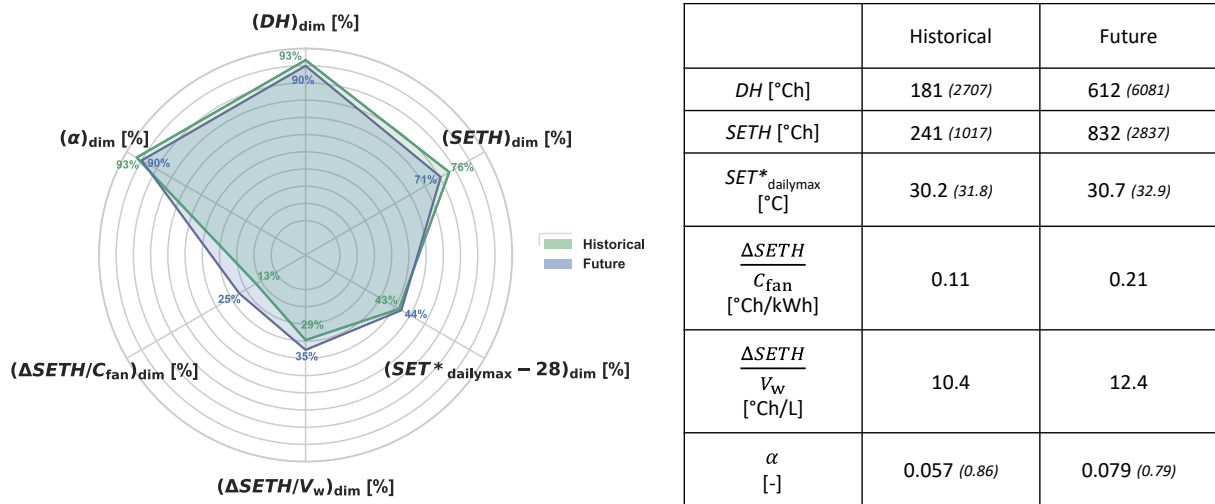


Figure 6 : System performance for two climate periods

Figure 6 show that the system performs equally well in historical and future climate conditions. The relative values obtained compared with the reference case (without system) show little difference in the system impact on reducing indoor overheating between the two climate periods. Nevertheless, the performance results ( $\Delta SETH/V_w$  and  $\Delta SETH/C_{fan}$ ) show that the system has a better impact in future climate conditions with respectively 12 and 6 points more reduction than in the historical climate. In absolute terms, we can see that the number of degree hours ( $DH$ ) remains high for the typical future period (612 °Ch), more than 3 times higher than the typical historical period (181 °Ch). This phenomenon is more significant when we look at the  $SETH$ , which is due to the increase in outdoor temperatures at night and during the day. As a result, the maximum daily average occupancy of  $SET^*$  for the year is 30.7 °C for the future period and 30.2 °C for the historical period. It can also be seen that the system is well adapted to climate change, particularly by observing the resilience indicator  $\alpha$ , which remains low ( $\alpha < 1$ ), despite taking into account a typical future climate scenario.

Finally, we note that the reduction of internal overheating relative to fan consumption ( $\Delta SETH/C_{fan}$ ) is better for the future period (0.21 °Ch/kWh) than for the historical period (0.11 °Ch/kWh). The trend is similar if we relate the reduction of internal overheating to the volume of water evaporated ( $\Delta SETH/V_w$ ); we observe a 19% increase in this gain between the historical period (10.4 °Ch/L) and the future period (12.4 °Ch/L).

These results indicate that without a system, in both climate scenarios, the building is able to eliminate external thermal stress in the long term. However, this phenomenon is accentuated in the presence of the system. In terms of reducing indoor overheating, the system performs similarly between historical and future climate conditions. However, when this reduction is



related to the system consumption (water and fan), the system performance is better in future climate conditions. The system should be more efficient in the years to come, when outdoor conditions are more important.

## 4 CONCLUSION

The aim of this study was to assess the ability of a direct adiabatic cooling system integrated into an industrial building, located in a mediterranean climate, to meet the challenges of climate change. The results demonstrated the resilience and efficiency of the system under projected future climate conditions. Analysis of the system behaviour revealed an increase in the operating time of the adiabatic and free-cooling systems to face the increased external heat input, resulting in higher fan energy consumption and higher water consumption. In a future climate, the system adapted to maintain its effectiveness in mitigating indoor overheating compared with historical climate data. Despite an increase in the severity of external thermal conditions, the resilience indicator remained low. Finally, the system performed better under future climate conditions, with a significant reduction in indoor overheating compared with the energy consumption of the fan (+90%) and the volume of water evaporated (+19%).

## 5 REFERENCES

ASHRAE. 2013. « ANSI/ASHRAE Standard 55-2013 ».

Batiweb. 2023. « PAC : un marché en demi-teinte ». Batiweb. 2023. <https://www.batiweb.com/actualites/vie-des-societes/www.batiweb.com>.

Breteau, Antoine, Patrick Salagnac, Emmanuel Bozonnet, Mathieu Carage, et Jean-Marie Caous. 2022. « Evaluation des performances énergétiques d'un système de rafraîchissement adiabatique intégré au sein d'un bâtiment industriel ». In *Colloque International Franco-Québécois en Energie Ville et Transition face aux défis climatiques et énergétiques*, 164-69. Ville et Transition face aux défis climatiques et énergétiques. Paris, France. <https://hal.archives-ouvertes.fr/hal-03718248>.

Breteau, Antoine, Patrick Salagnac, Emmanuel Bozonnet, Mathieu Carage, et Jean-Marie Caous. 2023. « Comparaison d'indicateurs dans l'analyse du confort intérieur d'un bâtiment industriel équipé d'un système de rafraîchissement adiabatique direct ». In *31ème Congrès Français de la Société Française de Thermique "Thermique et Agroressources"*, 127. Reims, France: Société Française de Thermique. <https://doi.org/10.25855/SFT2023-127>.

Chiesa, Giacomo, Nora Huberman, David Pearlmutter, et Mario Grosso. 2017. « Summer Discomfort Reduction by Direct Evaporative Cooling in Southern Mediterranean Areas ». *Energy Procedia*, 8th International Conference on Sustainability in Energy and Buildings, SEB-16, 11-13 September 2016, Turin, Italy, 111 (mars): 588-98. <https://doi.org/10.1016/j.egypro.2017.03.221>.

Ford, Brian, Nimish Patel, Parul Zaveri, et Mark Hewitt. 1998. « Cooling without Air Conditioning: The Torrent Research Centre, Ahmedabad, India ». *Renewable Energy*, Renewable Energy Energy Efficiency, Policy and the Environment, 15 (1): 177-82. [https://doi.org/10.1016/S0960-1481\(98\)00150-5](https://doi.org/10.1016/S0960-1481(98)00150-5).

Gagge, A., A. Fobelets, et L. Berglund. 1986. « A standard predictive index of human response to the thermal environment ». *Ashrae Transactions* 92 (1): 709-31.

Hamdy, Mohamed, Salvatore Carlucci, Pieter-Jan Hoes, et Jan L. M. Hensen. 2017. « The Impact of Climate Change on the Overheating Risk in Dwellings—A Dutch Case Study ». *Building and Environment* 122 (septembre): 307-23. <https://doi.org/10.1016/j.buildenv.2017.06.031>.

Kowalski, Piotr, et Dariusz Kwiecień. 2020. « Evaluation of Simple Evaporative Cooling Systems in an Industrial Building in Poland ». *Journal of Building Engineering* 32 (novembre). <https://doi.org/10.1016/j.jobe.2020.101555>.

Machard, Anaïs, Christian Inard, Jean-Marie Alessandrini, Charles Pelé, et Jacques Ribéron. 2020. « A Methodology for Assembling Future Weather Files Including Heatwaves for Building Thermal Simulations from the European Coordinated Regional Downscaling Experiment (Euro-Cordex) Climate Data ». *Energies* 13 (13): 3424. <https://doi.org/10.3390/en13133424>.

Mckenzie, Erica, Theresa Pistochini, Frank Loge, et Mark Modera. 2013. « An investigation of coupling evaporative cooling and decentralized graywater treatment in the residential sector ». *Building and Environment* 68 (octobre): 215-24. <https://doi.org/10.1016/j.buildenv.2013.07.007>.

PROFEEL. 2021. « Les solutions de rafraîchissement adiabatique dans les bâtiments tertiaires en rénovation ». *Profeel* (blog). 2021. <https://programmeprofeel.fr/ressources/guide-les-solutions-de-rafraichissement-adiabatique-dans-les-batiments-tertiaires-en-renovation/>.

PROMEE. 2023. « La climatisation représente 5% des émissions de CO2 du bâtiment ». Promee. 2023. <http://promee.fr/actualites/conseils/la-climatisation-represente-5-des-emissions-de-co2-du-batiment>.

Sahai, Rashmi. 2012. « Addressing Water Consumption of Evaporative Coolers with Greywater », juillet. <https://escholarship.org/uc/item/6gz5q7mx>.

Salamanca, F., M. Georgescu, A. Mahalov, M. Moustauoui, et M. Wang. 2014. « Anthropogenic Heating of the Urban Environment Due to Air Conditioning ». *Journal of Geophysical Research: Atmospheres* 119 (10): 5949-65. <https://doi.org/10.1002/2013JD021225>.

Watt, John R. 1997. *Evaporative Air Conditioning Handbook*. 3rd ed. Lilburn, GA, Upper Saddle River, NJ: Fairmont Press.

WMO. 2024. « L'OMM confirme que 2023 bat le record mondial de températures ». Organisation Météorologique Mondiale. 12 janvier 2024. <https://wmo.int/fr/media/news/lomm-confirme-que-2023-bat-le-record-mondial-de-temperatures>.

Xuan, Y. M., F. Xiao, X. F. Niu, X. Huang, et S. W. Wang. 2012. « Research and Application of Evaporative Cooling in China: A Review (I) – Research ». *Renewable and Sustainable Energy Reviews* 16 (5): 3535-46. <https://doi.org/10.1016/j.rser.2012.01.052>.

Zare, Sajad, Naser Hasheminejad, Hossein Elahi Shirvan, Rasoul Hemmatjo, Keyvan Sarebanzadeh, et Saeid Ahmadi. 2018. « Comparing Universal Thermal Climate Index (UTCI) with Selected Thermal Indices/Environmental Parameters during 12 Months of the Year ». *Weather and Climate Extremes* 19 (mars): 49-57. <https://doi.org/10.1016/j.wace.2018.01.004>.

Zhang, Chen, Ongun Berk Kazanci, Ronnen Levinson, Per Heiselberg, Bjarne W. Olesen, Giacomo Chiesa, Behzad Sodagar, et al. 2021. « Resilient Cooling Strategies- a Critical Review and Qualitative Assessment ». *Energy and Buildings*, juillet, 111312. <https://doi.org/10.1016/j.enbuild.2021.111312>.